

## Correlation of Mass, Energy, and Angle in MeV-Neutron-Induced Fission of $U^{235}$ and $U^{238}$ †

J. W. MEADOWS

Argonne National Laboratory, Argonne, Illinois 60439

(Received 30 August 1968)

Mass-energy distributions were measured for fission of  $U^{235}$  induced by thermal and by 0.12-, 0.5-, and 6.0-MeV neutrons, and fission of  $U^{238}$  induced by 1.5- and 5.6-MeV neutrons. Concurrent measurements were made at  $7^\circ$ ,  $45^\circ$ , and  $90^\circ$  to the incident neutron beam. No dependence of the anisotropy on mass was observed, nor did the average mass values, the average total kinetic energies, or the widths of the distributions show any angular dependence. The average single-fragment energies and provisional masses are consistent with the assumption that in 6.0-MeV-neutron-induced fission of  $U^{235}$  the additional fission neutrons come predominantly from the light fragment.

### 1. INTRODUCTION

EARLY measurements of the angular distribution of fission fragments<sup>1</sup> showed that the more asymmetric mass divisions tended to be more anisotropic than those from symmetric mass divisions. This, coupled with the success of the Bohr theory of fission anisotropy,<sup>2</sup> suggested that the mass division and the anisotropy might be determined by the saddle-point transition states. However, Griffin<sup>3</sup>, in an analysis of the energy dependence of the fission anisotropy in terms of the Bohr theory, showed that this apparent relation of anisotropy and fragment mass could be the result of fission at different excitation energies due to prior emission of neutrons.

Although this explanation qualitatively accounts for the correlation of fission anisotropy and mass asymmetry at energies above the threshold for multi-chance fission, it does not exclude the possibility of some more basic connection. Griffin's analysis shows that only data on fission at well-defined excitation energies can determine if such a connection exists. Consequently, it is of interest to study the mass-energy-angle distribution of fragments from fission induced by particles with incident energies high enough to produce anisotropic angular distributions but below the threshold for second chance fission. The results of the measurements that have been made in this energy range have not exhibited a definite trend. The  $U^{235}(n, f)$  and the  $U^{238}(n, f)$  reactions<sup>4,5</sup> at incident neutron energies of 4 and 3 MeV, respectively, have shown an anisotropy dependent on the mass ratio. Similar results have been observed for the  $Ra^{226}(p, f)$  reaction,<sup>6</sup> but this may be

due to the presence of a small percentage of the  $(p, nf)$  reaction. On the other hand, studies of the  $Th^{232}(n, f)$  and the  $U^{234}(d, pf)$  reactions<sup>7,8</sup> have indicated no relation between the anisotropy and the mass ratio.

This paper presents the results of a series of measurements of neutron-induced fission of  $U^{235}$  and  $U^{238}$ . Measurements were made at average angles of  $7^\circ$ ,  $45^\circ$ , and  $90^\circ$  relative to the incident neutron direction, using the double-energy technique and solid state detectors. The incident neutron energies were thermal, 0.12, 0.5, and 6.0 MeV for  $U^{235}$  fission and 1.5 and 5.6 MeV for  $U^{238}$  fission. The data have been analyzed to obtain the mass-total kinetic energy distributions and examined for correlations with the fission angle.

### II. EXPERIMENTAL METHOD AND PROCEDURES

The schematic diagram shown in Fig. 1 illustrates the relative position of the neutron source, uranium deposit, and detectors used to collect most of the data. The measurements of  $U^{238}$  fission at 1.5-MeV neutron energy were made with only two detectors, one on each side of the uranium deposit. This arrangement was first oriented to detect fragments at  $0^\circ$  to the incident neutron direction, then rotated to detect fragments at  $80^\circ$ . This method proved to be too time consuming, so the remaining measurements were made with the arrangement shown in Fig. 1. The uranium deposits were 1 cm in diameter and had a surface density of  $\sim 120 \mu\text{g}/\text{cm}^2$ . The  $U^{235}$  deposits were made by evaporating uranium metal enriched to  $\sim 93\%$  onto  $\sim 130 \mu\text{g}/\text{cm}^2$  nickel foils. The  $U^{238}$  deposits were made in a similar manner, using uranium metal containing  $\sim 0.2\%$   $U^{235}$ . The amount of material deposited was obtained by  $\alpha$  counting, and the thicknesses of the nickel foils were estimated from the energy loss of  $\alpha$  particles passing through them. The two fission sources were arranged so they could be interchanged without disconnecting the detectors or opening the detector vacuum chamber.

† Work supported by the U.S. Atomic Energy Commission.

<sup>1</sup> B. L. Cohen, B. L. Ferrell-Bryan, D. J. Coombeond, and M. K. Hullings, *Phys. Rev.* **98**, 685 (1955).

<sup>2</sup> A. Bohr, in *Proceedings of the First International Conference on the Peaceful Uses of Atomic Energy, Geneva, 1956* (United Nations, New York, 1956), Vol. 2, p. 151.

<sup>3</sup> J. L. Griffin, *Phys. Rev.* **116**, 107 (1959).

<sup>4</sup> S. S. Kapoor, D. M. Nadkarni, R. Ramanna, and P. N. Rama Rao, *Phys. Rev.* **137**, 511B (1965).

<sup>5</sup> I. A. Baranov, A. N. Protopopov, and V. P. Eismont, *Zh. Eksperim. i Teor. Fiz.* **41**, 1003 (1961) [English transl.: *Soviet Phys.—JETP* **14**, 713 (1962)].

<sup>6</sup> H. W. Schmitt, J. W. T. Dabbs, and P. D. Miller, *Physics and Chemistry of Fission*, (International Atomic Energy Agency, Vienna, 1965), Vol. I, p. 517.

<sup>7</sup> B. D. Kuzminov and A. I. Sergachev, *Physics and Chemistry of Fission*, (International Atomic Energy Agency, Vienna, 1965), Vol. I, p. 611.

<sup>8</sup> R. Vandenbosch, J. P. Unik, and J. R. Huizenga, *Physics and Chemistry of Fission*, (International Atomic Energy Agency, Vienna, 1965), Vol. I, p. 547.

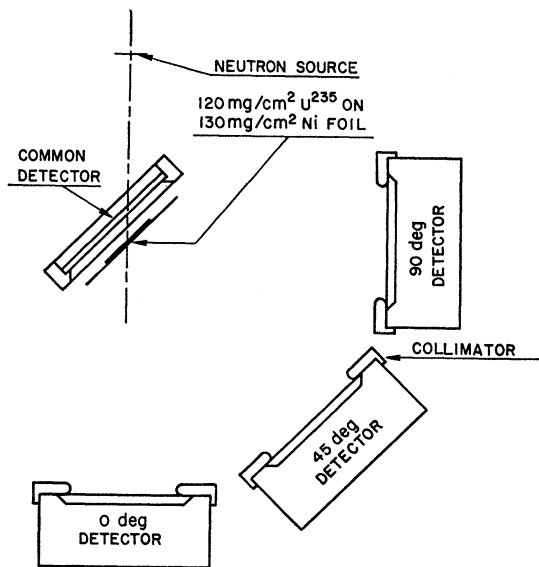


FIG. 1. Schematic diagram of the relative positions of the neutron source, fission source, and detectors.

Neutrons were produced by the  $D(d, n)He^3$  and the  $Li^7(p, n)Be^7$  reactions using deuterium gas and thin lithium metal targets bombarded with ions from a 3-MeV Van de Graaff generator. Target thicknesses were adjusted so the neutron energy spreads were  $\sim 100$  keV from the gas targets and  $\sim 50$  keV from the metal targets. Thermal neutrons were obtained by encasing the detector chamber in about 4 in. of paraffin.

Most of the measurements were made with silicon surface barrier detectors having room-temperature resistivities in the vicinity of  $500 \Omega$  cm. The active areas were  $4 \text{ cm}^2$  for the common detector and  $3 \text{ cm}^2$  for the others. The edges of the detectors were shielded by aluminum collimators whose inside edges were rounded to minimize scattering. Silicon diffuse junction detectors with  $2\text{-cm}^2$  areas and similar collimators were used to measure  $U^{238}$  fission at 1.5 MeV. All detectors were operated at a bias high enough to insure saturation, usually about 70 V.

Since the detectors were exposed to high fluxes of fast neutrons, radiation damage was a major problem. This was particularly true of the common detector which was located very close to the neutron source. During the course of these experiments, two detectors were bombarded with 6-MeV neutrons and their behavior was followed until they failed as spectrometers. The detector biases were kept within  $\pm 1$  V of their nominal values and  $U^{235}$  thermal-fission spectra were recorded at intervals. The room-temperature reverse current increased at the rate of  $\sim 0.6 \mu\text{A}/10^{12}$  neutrons. The pulse height decreased at the rate of  $\sim 0.5\%/10^{12}$  neutrons/cm<sup>2</sup> or  $\sim 0.04\%/h$  under the conditions of this experiment. The detectors continued to act as good spectrometers for fission fragments until the exposure reached  $\sim 10^{13}$  neutrons/cm<sup>2</sup> when the rate of pulse

height decrease suddenly went up by an order of magnitude and the fission spectra began to show obvious distortions.

In order to reduce the problem of high reverse currents and their fluctuations caused by temperature changes in the target room, the temperature of the detectors was reduced and stabilized by cooling the walls of the detector vacuum chamber. The chamber was wrapped in a thin polyethylene sheet to provide insulation and to prevent condensation. Four similar charge-sensitive preamplifier-amplifier systems were used to amplify the detector pulses. When a pair of fission fragments were detected simultaneously in the common detector and one of the other detectors, the event was recorded in a  $64 \times 64$  array appropriate to the detector combination. The rows of the array represented the pulse height from one fragment and the columns of pulse height from the other. Amplifier gains and zero levels were adjusted so the 64 channels covered the energy interval from  $\sim 40$  to  $\sim 120$  MeV. The average angles of the fission fragments detected by the three detector combinations were  $7^\circ$ ,  $45^\circ$ , and  $90^\circ$  with distributions having full widths at half maximum of  $4^\circ$ ,  $7^\circ$ , and  $9^\circ$ , respectively. Fast-neutron fission data were collected in a series of runs averaging 4 hours each with about 18 runs being made at each energy. Thermal-fission spectra were collected for 2-h periods at least once each 24 hours to provide the energy calibration and the thermal-fission data. Pulsar measurements to confirm the stability of amplifier gains and zero levels were made after every second run. Typical count rates were  $\sim 10$  (counts/min)/(detector pair) for fast-neutron fission and  $\sim 200$  (counts/min)/(detector pair) for thermal fission. The order of the measurements and the approximate number of fissions collected at each angle were: (1)  $U^{238}$ , 1.5 MeV, 7000; (2)  $U^{235}$ , 6.0 MeV, 45 000; (3)  $U^{238}$ , 5.6 MeV, 15 000; (4)  $U^{235}$ , 0.12 MeV, 37 000; (5)  $U^{235}$ , 0.5 MeV, 21 000.

### III. ANALYSIS

The relation between the initial and final energies of a fission fragment with respect to neutron emission has been discussed by Terrell<sup>9</sup> and Schmitt *et al.*<sup>10</sup> The conservation of mass and momentum leads to the relation

$$m_2^* = A E_1^* / (E_1^* + E_2^*), \quad (1)$$

where  $m_i^*$  is the fragment mass before neutron emission,  $E_i^*$  is the corresponding energy,  $A$  is the mass of the fissioning nucleus, and  $i$  identifies the detector. If recoil effects are neglected the energy of the fragment after emitting  $\nu_1$  neutrons is

$$E_i = E_i^* - (\nu_1 E_i^* / m_i^*). \quad (2)$$

This is the quantity measured by the double-energy

<sup>9</sup> J. Terrell, Phys. Rev. **127**, 880 (1962).

<sup>10</sup> H. W. Schmitt, J. H. Neiler, and F. J. Walter, Phys. Rev. **141**, 1146 (1966).

technique. The second term in Eq. (2) is usually small and replacing  $E_i^*$  by  $E_i$  in Eq. (1) gives "mass" values which are near but not usually equal to the true values. Following Schmitt *et al.*<sup>10</sup> such "mass" values are termed "provisional" masses,  $\mu_i$ .

Terrell<sup>9</sup> has shown that the provisional mass distribution will be broader than the preneutron emission mass distribution owing to (1) the correlation of  $\nu_i$  and  $m_i^*$ , (2) the distribution in  $\nu_i$  from a given  $m_i^*$ , and (3) the recoil effects of the emitted neutrons. For thermal-neutron-induced fission of U<sup>235</sup>, the variance of the preneutron emission mass distribution,  $\sigma^2(m_H^*)$ , is  $\sim 30$  amu<sup>2</sup>. Because of the effects of neutron emission, the variance of the provisional mass distribution,  $\sigma^2(\mu_H)$ , is  $\sim 35$  amu<sup>2</sup>.

Experimental effects also contribute but to a lesser extent. A detector resolution of  $\sim 1.5$  MeV for fission fragments will increase  $\sigma^2(\mu)$  by  $\sim 0.4$  amu<sup>2</sup>. In the method used in this experiment, the variation in the energy loss by the fragments in the support foil and detector windows, due to the distribution in the angle of incidence, increases  $\sigma^2(\mu)$  for the 7° and 90° distributions by  $\sim 1$  amu<sup>2</sup>. At 45° where the fragments enter nearly normal to all absorbing layers the increase in width is negligible.

The major problem in data reduction was the transformation of the pulse-height array,  $N(X_1, X_2)$ , into a provisional mass versus total kinetic energy array,  $N(\mu_2, E_k)$ . This problem has been discussed by Thomas and Gibson.<sup>11</sup> Because of the low statistical accuracy of most of the data, a variation of their subcell method was used. The final array was divided into cells 1.2 amu by 1.5 MeV and the corners of each of these cells were transformed onto the  $(X_1, X_2)$  array. The cells which were covered or partly covered were identified and the number of events recorded in these cells were entered in the  $(\mu_2, E_k)$  cell according to the fraction of coverage.

The equations relating the two arrays are listed below. In the following equations the provisional mass is used in all terms involving mass. However, since it is not greatly different from the true mass, the error introduced is negligible.

$$E_i' = (a + a'\mu_i)X_i + b + b'\mu_i + cE_i^{1/3}, \quad (3)$$

$$E_i = E_i'(1 + \rho_i^2 - 2\rho_i \cos\theta_i), \quad (4)$$

$$\rho_i = [(m_n \mu_i E_n) / (A^2 E_i)]^{1/2}, \quad (5)$$

$$\mu_2 = A E_1 / E_k, \quad (6)$$

$$E_k = E_1 + E_2. \quad (7)$$

Equation (3) relates the energy in the laboratory system,  $E_i'$ , of a fragment detected by the  $i$ th detector to the corresponding pulse height,  $X_i$ . The constants  $a$ ,  $a'$ ,  $b$ , and  $b'$  were calculated from measurements of the U<sup>235</sup> thermal neutron fission spectrum according

<sup>11</sup> T. D. Thomas and W. M. Gibson, Proceedings of the Conference on Utilization of Multiparameter Analyzers in Nuclear Physics, Report No. NYO 10595, 1963 (unpublished).

to the method of Schmitt *et al.*<sup>12</sup> These calibration constants also compensate for the energy lost by the fragments in the detector windows, fission source, and support foil. The last term of Eq. (3) corrects for the difference in the energy lost in the fission source when the one being measured is not the same as the one used for calibration. This correction was based on measurements by Alexander and Gazdik.<sup>13</sup> More recent theoretical studies<sup>14</sup> show that the initial rate of energy loss is more nearly given by  $kE^{1/2}$  where  $k$  is a function of fragment mass. Experimental measurements<sup>15</sup> show that  $k$  also has some energy dependence. However, when the correlation of fragment mass and energy is considered, the form of the correction used is a fair approximation for small energy losses. In the U<sup>238</sup> measurements this correction amounted to  $\sim 1.5 \pm 0.5$  MeV for the average fragment.

Equations (4) and (5) transform the laboratory energy of the fragment to its c.m. energy.  $E_n$  and  $m_n$  are the energy and mass of the incident neutron and  $\theta_i$  is the laboratory angle of the fission fragment relative to the incident neutron direction. Finally, Eqs. (6) and (7) relate the provisional mass and total kinetic energy to the fragment energies after neutron emission.

In the usual processing procedure, all runs, including the pulser and calibration runs, for a given series of measurements were examined for unusual gain shifts. If there were any, all neighboring runs were discarded. Next, a set of constants for Eq. (3) was obtained for each thermal calibration run, and linear interpolations were used to obtain constants for the intervening runs. After making the transformations to the  $N(\mu_2, E_k)$  arrays, all the results at each energy and angle were added together. In order to test for experimental and processing errors the appropriate U<sup>235</sup> calibration data were always processed concurrently with the other measurements.

All the data reported in this paper are in terms of provisional mass values and post-neutron emission energies, and have not been corrected for experimental dispersions. If the relation between  $\nu_i$  and  $m_i^*$  and the distribution of  $\nu_i$  are known, then the preneutron emission mass distribution can be deduced from the provisional mass distribution. This has been done<sup>10</sup> for spontaneous fission of Cf<sup>252</sup> and thermal neutron fission of U<sup>235</sup> where the dependence of  $\nu_i$  on  $m_i^*$  is known but this quantity has not been measured for fast-neutron fission. The dispersion caused by experimental effects is relatively small compared to that caused by neutron emission so there was little to be gained by making this correction.

<sup>12</sup> H. W. Schmitt, W. M. Gibson, J. H. Neiler, F. J. Walter, and T. O. Thomas, *Physics and Chemistry of Fission*, (International Atomic Energy Agency, Vienna, 1965), Vol. I, p. 531.

<sup>13</sup> J. M. Alexander and M. F. Gazdik, *Phys. Rev.* **120**, 874 (1960).

<sup>14</sup> J. Lindhard, M. Scharff, and H. E. Schiott, *Kgl. Danske Videnskab Selskab, Mat. Fys. Medd.* **33**, No. 14 (1963).

<sup>15</sup> M. S. Moore and L. G. Miller, *Phys. Rev.* **157**, 1049 (1967).

TABLE I. Mean values and widths of the distributions. The symbols  $\bar{\mu}_L$  and  $\bar{\mu}_H$  are the average provisional masses of the light and heavy peaks,  $\bar{E}_L$  and  $\bar{E}_H$  are the average energies of the light and heavy fragments, and  $\bar{E}_k$  is the average total kinetic energy. The energies are measured relative to the  $U^{235}$  thermal-neutron fission spectrum, and the errors are relative to this standard. The symbol  $Y_s$  represents the yield at symmetry with its statistical error averaged over an interval 4.8 amu wide. No corrections have been made for neutron emission or dispersion effects

| $E_n$<br>MeV | $\theta$<br>deg | $\bar{\mu}_L$<br>amu | $\bar{\mu}_H$<br>amu | $\sigma^2(\mu)$<br>amu <sup>2</sup> | $\bar{E}_L$<br>MeV | $\bar{E}_H$<br>MeV | $\bar{E}_k$<br>MeV | $Y_s$<br>%                   |
|--------------|-----------------|----------------------|----------------------|-------------------------------------|--------------------|--------------------|--------------------|------------------------------|
| $U^{235}$    |                 |                      |                      |                                     |                    |                    |                    |                              |
| Thermal      | 7               | 97.2                 | 139.1                | 34.7                                | 100.2              | 70.3               | 170.5              | 0.020±0.002                  |
|              | 45              | 97.2                 | 139.1                | 33.5                                | 100.2              | 70.2               | 170.4              | 0.020±0.002                  |
|              | 90              | 97.4                 | 139.1                | 34.9                                | 100.2              | 70.4               | 170.6              | 0.020±0.002                  |
| 0.12         | 7               | 97.2                 | 138.9                | 35.0                                | 99.8±0.2           | 70.1±0.3           | 170.0±0.4          | 0.013±0.003                  |
|              | 45              | 97.5                 | 138.6                | 33.4                                | 99.8±0.2           | 70.3±0.3           | 170.2±0.4          | 0.016±0.003                  |
|              | 90              | 96.8                 | 138.7                | 35.0                                | 100.2±0.2          | 70.3±0.3           | 170.5±0.4          | 0.014±0.003                  |
| 0.5          | 7               | 97.3                 | 138.8                | 35.7                                | 99.8±0.3           | 70.1±0.3           | 169.9±0.4          | 0.017±0.004                  |
|              | 45              | 97.5                 | 138.4                | 33.6                                | 99.8±0.3           | 70.5±0.3           | 170.3±0.4          | 0.021±0.005                  |
|              | 90              | 97.0                 | 138.7                | 35.4                                | 100.0±0.3          | 70.2±0.3           | 170.3±0.4          | 0.024±0.005                  |
| 6.0          | 7               | 98.0                 | 138.6                | 46.5                                | 99.0±0.1           | 70.2±0.2           | 169.2±0.2          | 0.26±0.02                    |
|              | 45              | 98.0                 | 138.6                | 45.6                                | 98.9±0.1           | 70.1±0.2           | 169.0±0.2          | 0.26±0.02                    |
|              | 90              | 97.9                 | 138.2                | 46.1                                | 99.1±0.1           | 70.4±0.2           | 169.5±0.2          | 0.26±0.02                    |
| $U^{238}$    |                 |                      |                      |                                     |                    |                    |                    |                              |
| 1.5          | 7               | 100.2                | 139.0                | 37.0                                | 99.0±0.7           | 71.2±0.7           | 170.2±1.0          | 0.016±0.010<br>(0.015±0.007) |
|              | 80              | 99.9                 | 138.9                | 37.0                                | 99.2±0.7           | 71.6±0.7           | 170.8±1.0          | 0.024±0.011<br>(0.021±0.007) |
| 5.6          | 7               | 99.9                 | 139.5                | 43.4                                | 97.7±0.5           | 70.2±0.5           | 167.9±0.7          | 0.10±0.01                    |
|              | 45              | 99.6                 | 139.0                | 42.4                                | 97.8±0.5           | 70.3±0.5           | 168.1±0.7          | 0.09±0.01                    |
|              | 90              | 99.6                 | 139.2                | 42.8                                | 97.2±0.5           | 69.9±0.5           | 167.0±0.7          | 0.12±0.01                    |

#### IV. INCIDENT NEUTRON ENERGIES

The basic neutron bombardment energies in this experiment were 6.0 MeV for the  $U^{235}(n, f)$  reaction and 5.6 MeV for the  $U^{238}(n, f)$  reaction. The choice of these two energies was simple. They are high enough to provide a large number of fission channels combining both intrinsic and collective excitations, and the amount of symmetric fission is large enough to obtain reasonable statistical accuracy in the data. At higher energies, fission cross-section<sup>16</sup> and anisotropy<sup>17</sup> measurements suggest that the  $(n, n'f)$  reaction begins to be important. Measurements were also made at thermal, 0.12, and 0.5 MeV for the  $U^{235}(n, f)$  reaction and at 1.5 MeV for the  $U^{238}(n, f)$  reaction. These energies were chosen to emphasize fission through specific channels. The considerations that governed their choice are discussed in the next few paragraphs.

The capture of a neutron by  $U^{235}$  produces the even-even compound nucleus  $U^{236*}$ . Griffin<sup>18</sup> has suggested that the gap found in even-even nuclei between the ground state and the two quasiparticle threshold in-

creases to  $\sim 2.6$  MeV at the saddle point. If such is the case, all the fission channels appearing within this gap must be associated with transition states involving collective excitations. The ground state will have positive parity and  $K$ , the projection of the nuclear spin on the symmetry axis, will be equal to 0. The first excited state<sup>19</sup> is expected to have negative parity and  $K=0$ . The two lowest thresholds observed in the  $U^{235}(d, pf)$  reaction<sup>20</sup> are identified with these states placing them at  $E_n \sim -0.6$  MeV and  $E_n \sim 0.2$  MeV, respectively. Measurements of the energy dependence of the average total kinetic energy of the fission fragments, and of the average number of neutrons emitted per fission, are consistent with this interpretation, and also suggest that additional channels become available at  $E_n \sim 0.4$  MeV.<sup>21,22</sup> This is approximately where the

<sup>16</sup> J. R. Stehn, M. D. Goldber, R. Wiener-Chasman, S. F. Mughabghab, B. A. Magurno, and V. M. May, Brookhaven National Laboratory Report No. BNL-325 (1965) 2nd ed., Suppl. No. 2, Vol. III.

<sup>17</sup> J. E. Simmons and R. L. Henkel, Phys. Rev. **120**, 198 (1960).

<sup>18</sup> J. J. Griffin, Phys. Rev. **132**, 2204 (1963).

<sup>19</sup> Transition state spectra have been suggested by: J. A. Wheeler, *Fast Neutron Physics*, (Interscience Publishers, New York, 1963), Part II, p. 2051. J. J. Griffin, *Physics and Chemistry of Fission*, (International Atomic Energy Agency, Vienna, 1965), Vol. I, p. 23. J. G. Cuninghame, K. Fritze, J. E. Lynn, and C. B. Webster, Nucl. Phys. **84**, 49 (1966).

<sup>20</sup> J. A. Northrop, R. H. Stokes, and K. Boyer, Phys. Rev. **115**, 1277 (1959).

<sup>21</sup> Yu. A. Blyumkina, I. I. Bondarenko, V. F. Kutnaxov, V. G. Nesterov, B. N. Okolvich, G. N. Smirenkin, and L. N. Usachev, Nucl. Phys. **52**, 648 (1964).

<sup>22</sup> J. W. Meadows and J. F. Whalen, J. Nucl. Energy, **21**, 157 (1967).

next two transition states are expected to be.<sup>19</sup> There is disagreement on the order of their appearance but one is expected to be associated with a bending vibration with negative parity and  $K=1$  and the other with a  $\gamma$  vibration with positive parity and  $K=2$ .

The measurements at thermal energies were made to calibrate the detectors, and to provide a reference mass-energy distribution to which the other measurements could be compared. Since the spin and parity of the  $U^{235}$  ground state is  $\frac{7}{2}^-$  and because only  $s$ -wave neutrons are important, thermal-neutron fission can proceed only through the negative parity channel at  $E_n \approx 0.2$  MeV and the resulting angular distribution is isotropic.

The principal requirement of the second energy was that it be high enough to produce a large amount of  $p$ -wave fission in order to emphasize the effects of the positive parity channels. The behavior of the cross section of the  $Li^7(p, n)Be^7$  reaction made  $E_n=0.12$  MeV the most convenient choice. At this energy, optical model transmission coefficients<sup>23</sup> indicate that  $p$ -wave neutrons account for about 75% of the compound nucleus formation. Therefore, fission is expected to proceed primarily through the positive parity ground state.

The third energy,  $E_n=0.5$  MeV, was chosen because of the increased possibility of fission through channels with  $K>0$ . Since  $p$ -wave neutrons still account for  $\sim \frac{2}{3}$  of the compound nucleus formation, the positive parity channel with  $K=2$  was expected to be particularly important.

The saddle-point level structure for  $U^{238}+n$  is not so well defined. Because the target nucleus has zero spin and  $l_z=0$ ,  $M$  is limited to values of  $\pm \frac{1}{2}$  for neutron-induced fission so that the anisotropy is much more pronounced. Lamphere's analysis of the low-energy angular anisotropy<sup>24</sup> shows that fission initially occurs through  $K=\frac{1}{2}$  channels although others of larger  $K$  must also be present. As the compound nucleus is even-odd, the large pairing gap is not present and the first excited state involving intrinsic excitation may be close to the fission threshold. It is possible that the lowest neutron energy chosen,  $E_n=1.5$  MeV, is above this level, but the rapidly decreasing fission cross section<sup>25</sup> made it impractical to go to a lower energy.

## V. DISCUSSION

The results are summarized in Table I which lists the average masses, average energies, variances of the distributions, and normalized yields for symmetric mass division of all the measurements. The energies are all measured relative to the  $U^{235}$  thermal-neutron fission spectrum and only relative errors are quoted. For the  $U^{238}$  measurements, these errors are based

<sup>23</sup> P. A. Moldauer, Argonne National Laboratory Report, ANL-6323, March 1961 (unpublished).

<sup>24</sup> R. W. Lamphere, *Physics and Chemistry of Fission*, (International Atomic Energy Agency, Vienna, 1965), Vol. I, p. 63.

<sup>25</sup> S. Katcoff, *Nucleonics*, **18**, No. 11, 301 (1960).

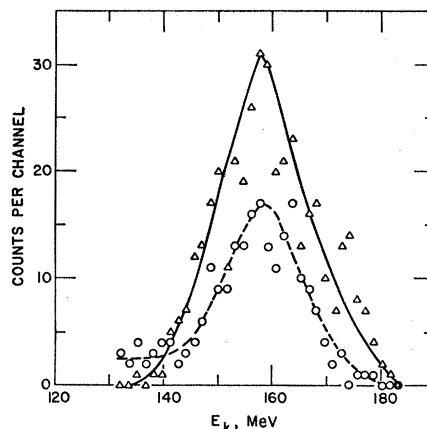


FIG. 2. Yield at symmetry versus total kinetic energy for the mass interval 116.8–119.2 for thermal and 6.0-MeV-neutron-induced fission of  $U^{235}$ . The total number of events of all mass divisions was  $\sim 10^6$  for thermal fission and  $\sim 10^5$  for 6.0-MeV fission.

entirely on the scatter of the results from the several runs at each neutron energy. For the  $U^{238}$  measurements, they include the 0.5-MeV error due to the difference in the thickness of the fission sources discussed in Sec. III. Unfortunately, the original foil was broken after the 1.5 MeV measurements so this error must also be considered when the relative energies of the two  $U^{238}$  measurements are discussed. The yields for symmetric mass division  $Y_s$  and their errors are based on the number of events recorded in the two channels on either side of the point of equal mass division.

The calculated values of  $\bar{\mu}_L$  and  $\bar{\mu}_H$  do not usually sum exactly to the mass of the fissioning nucleus. This is partly due to the uncertainty introduced by the coarseness of the arrays, the method of processing which assumes a constant distribution across a cell, and also to the sensitivity of the results to the location of the calibration points. For example, an error of half a channel in the location of one of the heavy mass peaks can cause an error of  $\sim 0.5$  amu in  $\bar{\mu}_L$  and an error of  $\sim 1.5$  amu<sup>2</sup> in  $\sigma^2(\mu_L)$ .

The value of  $Y_s$  for thermal-neutron fission of  $U^{235}$  provides a criterion for judging the validity of the mass-energy distributions since the region around symmetric mass division is particularly subject to distortion. The observed value of  $Y_s$  is 0.020% which may be compared to the radiochemical<sup>25</sup> value of 0.01%. Some increase in  $Y_s$  is expected because of the dispersion effects due to neutron emission and detector resolution. In addition, the light fragment may lose energy by scattering in the relatively thick uranium deposit and nickel foil so that it has about the same energy as the heavy fragment. Since  $E_H \approx 70$  MeV,  $E_k$  for these events is  $\sim 140$  MeV. The magnitude of the increase in  $Y_s$  is expected to be about the same for all these measurements because of the similarity of the mass-energy distributions and of the experimental equipment and

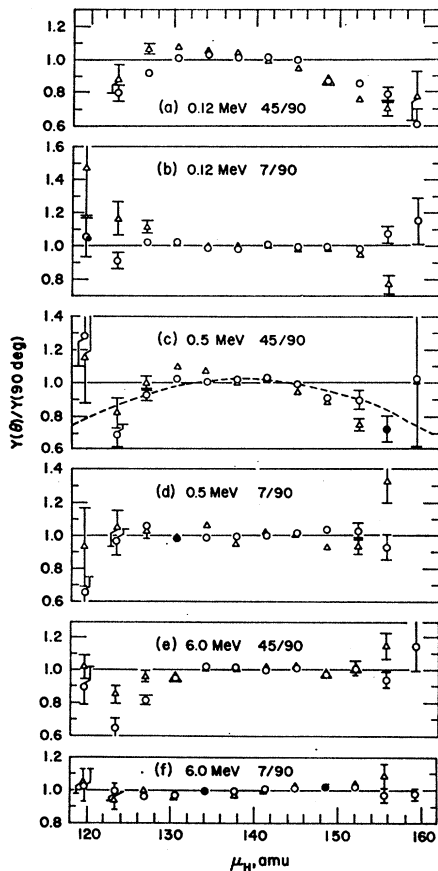


FIG. 3. The mass dependence of the ratios of the yields at 7° and 45° to the yield at 90° for neutron-induced fission of  $U^{235}$ . The data represented by  $\Delta$  are at the indicated energies while the  $\circ$  give the results of the corresponding thermal-calibration measurements. Each point represents an interval 3.6-amu wide. See the text for the explanation of the apparent mass-angle correlation of the 45°-90° ratio.

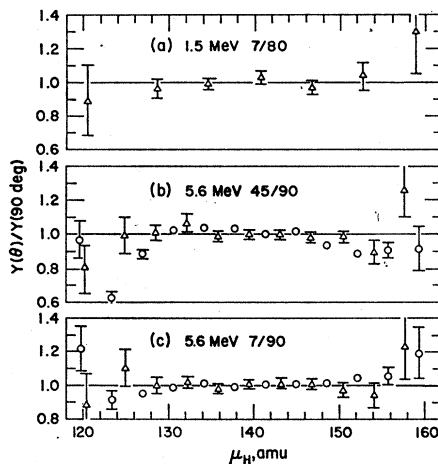


FIG. 4. The mass dependence of the ratio of the yields at 7° and 45° to the yield at 90° for neutron-induced fission of  $U^{235}$ . The data represented by  $\Delta$  are at the indicated energies while the  $\circ$  give the results of the corresponding  $U^{235}$  thermal-calibration measurements. Each point represents an interval 6.1 amu wide in the 1.5-MeV data and 3.6-amu wide in the 5.6-MeV data. See the text for the explanation of the apparent mass-angle correlation of the 45°-90° ratio.

procedures. At incident neutron energies of 5.6 and 6.0 MeV where  $Y_s$  has increased by an order of magnitude such effects are expected to be negligible. The distribution of  $E_k$  near symmetry for thermal and 6.0-MeV fission of  $U^{235}$  is plotted in Fig. 2. The thermal data do show a relatively large number of events at  $E_k \sim 140$  MeV. Their number suggests that  $\sim 30\%$  of the thermal symmetric events may be due to energy degradation. This is in reasonable agreement with the radiochemical data which indicate that  $\sim 50\%$  of  $Y_s$  is due to dispersion effects and energy degradation.

The data in Table I show no angular dependence outside experimental error. The value of  $\sigma^2(\mu)$  at 45° is consistently less than the value at the other angles by about one unit, but this also appears in the thermal measurements and is caused by a systematic effect discussed in Sec. III. The mass dependences of the yield

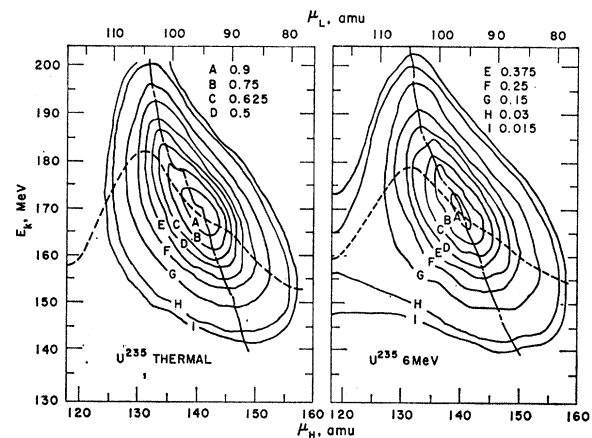


FIG. 5. Contour plot of the provisional mass versus total kinetic energy array  $N(\mu, E_k)$  for thermal and 6-MeV-neutron-induced fission of  $U^{235}$ . The long-short dashed curve indicates the location of the most probable mass versus  $\mu_H$ , while the dashed curve shows the location of the most probable energy.

ratios  $Y(\mu, \theta)/Y(\mu, 90)$  are shown in Figs. 3 and 4. In order to show the existence of any systematic errors the yield ratios of the corresponding thermal-calibration measurements are plotted on the same graphs.  $Y(\mu, 7)/Y(\mu, 90)$  does not show a statistically significant departure from 1.0 in any measurement. This is particularly evident in the higher-energy data shown in Figs. 3(f) and 4(c), where good statistical accuracy extends into the region of symmetric fission. Even when some small systematic deviations do appear, they are repeated in the associated calibration measurements which shows that they are caused by experimental effects. The plots of  $Y(\mu, 45)/Y(\mu, 90)$  show an apparent mass dependence, but the agreement with the calibration measurements shows that this is an experimental effect. To illustrate this, the ratio of two Gaussian distributions with the values of  $\sigma^2(\mu)$  corresponding to the experimental values in Table I is plotted in Fig. 3(c). The agreement with the data shows that the apparent mass dependence is caused

by the angular dependence of  $\sigma^2(\mu)$  discussed in Sec. III.

Since no angular correlation was observed the data from the  $7^\circ$  and  $90^\circ$  measurements were summed and the resulting  $N(\mu_H, E_k)$  arrays for thermal and 6.0-MeV-neutron fission of  $U^{235}$  and for 1.5- and 5.6-MeV-neutron fission of  $U^{238}$  are shown as contour plots in Figs. 5 and 6. The mass dependence of the fission yield, average single-fragment kinetic energy, and average total kinetic energy are shown in Figs. 7 and 8. The corresponding results for the 0.12- and 0.5-MeV-neutron fission of  $U^{235}$  are not shown as the data are too similar to the thermal results for any differences to appear.

The positions of the most probable mass and most probable energy as functions of  $\mu_H$  are also shown in Figs. 5 and 6. For  $U^{235}$  thermal-neutron fission the most probable mass curve shows two distinct steps at  $\mu_H=136$  and  $\mu_H=140$ . These do not appear in the 6-MeV data but there is some indication of a similar effect in both the 1.5- and 5.6-MeV fission of  $U^{238}$ . A mass of 136 is very near the  $N=82$ ,  $Z=50$  shells. On the other hand  $\mu_H=140$  is well removed from these shells and its complementary fragment,  $\mu_L=96$ , is not near the  $N=50$  shell. In Fig. 6 the contour plot for 1.5 MeV  $U^{238}$  fission shows the possibility of structure on the side of the mass peak and also a double peak which persists at 5.6 MeV. The presence of this double peak is not especially certain at either energy because of the limited statistical accuracy. However, its appearance at both energies is good evidence of its actual existence.

Table I shows that small increases in the incident neutron energy have little effect on the shape of the mass peaks. However, the higher energies show a very significant increase in  $\sigma^2(\mu)$  of which only about one unit can be attributed to increased neutron emission unless there is a very large change in  $dv/dm^*$ . Much of the increase in  $\sigma^2(\mu)$  is caused by the increased yield

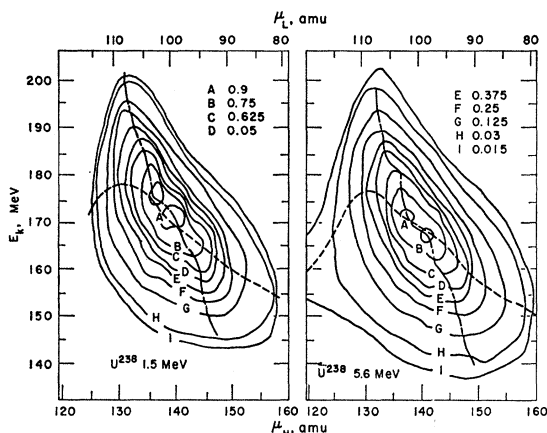


FIG. 6. Contour plot of the provisional mass versus total kinetic-energy array  $N(\mu, E_k)$  for 1.5 and 5.6-MeV-neutron-induced fission of  $U^{238}$ . The long-short dashed curve indicates the location of the most probable mass versus  $\mu_H$  while the dashed curve shows the location of the most probable energy.

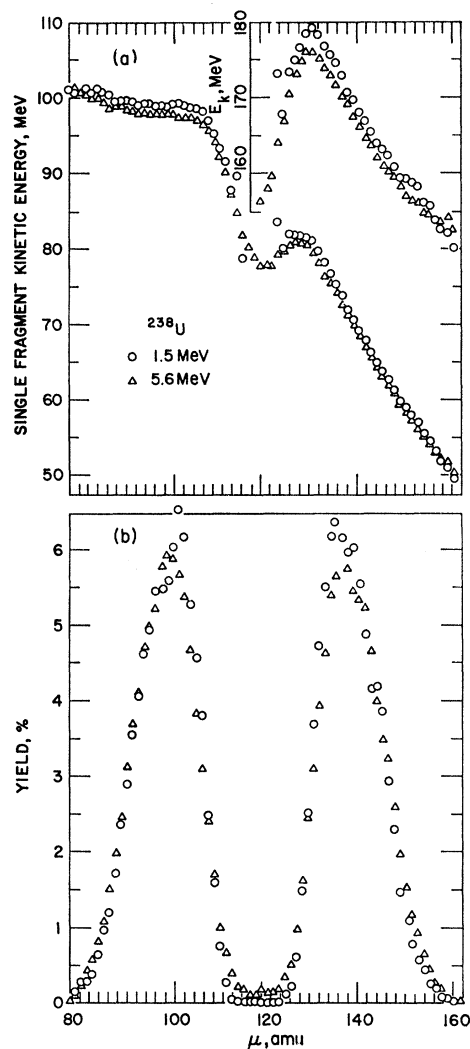


FIG. 7. Results for thermal and 6.0-MeV-neutron-induced fission of  $U^{235}$ . (a) Average fragment kinetic energy and average total kinetic energy versus provisional mass; (b) yield versus provisional mass.

at symmetry and, to a lesser extent, by an increase in very asymmetric fission.

Another point of interest in these measurements is the dependence of  $Y_s$  on the incident neutron energy. As mentioned above, radiochemical measurements suggest that where  $Y_s$  is small a significant part may be due to false events. It should be remembered that radiochemical measurements give yields after neutron emission, while the double-energy measurements give a first-order approximation of the yields before neutron emission. However, radiochemical measurements are not affected by detector resolution, neutron recoils, or fragment energy losses, so for the following discussion it is assumed that for thermal-neutron fission of  $U^{235}$  the radiochemical result,<sup>25</sup>  $Y_s=0.01\%$ , is the true value. The corresponding result from Table I, averaged over all three angles, is  $(0.020 \pm 0.001)\%$ . Thus the increase in  $Y_s$  due to false events is  $0.01\%$ .

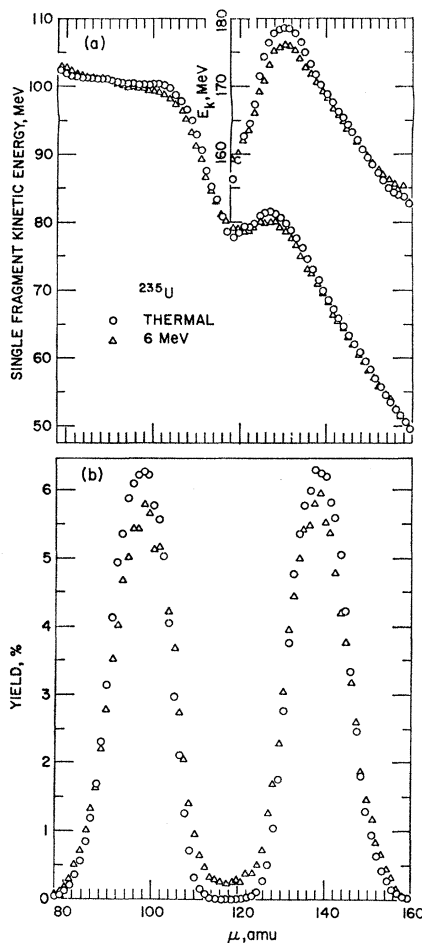


FIG. 8. Results for 1.5 and 5.6-MeV-neutron-induced fission of  $U^{238}$ . (a) Average fragment kinetic energy and average total kinetic energy versus provisional mass; (b) yield versus provisional mass.

It is also assumed that this same correction is applicable to the data for other incident neutron energies because of the similarity of the mass-energy distributions and the experimental procedures. After applying this correction,  $Y_s$  for fission of  $U^{235}$  by 0.5-MeV neutrons becomes  $(0.011 \pm 0.003)\%$  or nearly the same as the thermal value. For 0.12 MeV neutron energy the corrected  $Y_s$  is  $(0.004 \pm 0.002)\%$ . These results are in qualitative agreement with the radiochemical data of Cuninghame *et al.*<sup>26</sup> who showed that the symmetric fission yield of  $U^{235}$  decreased by a factor of 2 with the onset of *p*-wave fission but returned to the thermal value near 0.5-MeV-neutron energy.

Two sets of values of  $Y_s$  are listed in Table I for 1.5-MeV-neutron fission of  $U^{238}$ . The first set of values includes only the data used in determining the mass-

energy distributions. However, about half the data collected for this measurement was not used because the bias voltage of one of the detectors was permitted to shift too far from the nominal value. While this may have affected the mass-energy distribution to some extent, it is unlikely to have caused a significant error in  $Y_s$ . The values of  $Y_s$  obtained when all the data were used are listed in Table I in parentheses. Although the statistical accuracy is improved, the error is still very large. If the data from both angles are used and the contribution from false events is assumed to be 0.01, then  $Y_s$  for 1.5-MeV fission of  $U^{238}$  is  $(0.008 \pm 0.005)\%$ .

The yield near symmetry for 6.0-MeV fission of  $U^{235}$  and 5.6-MeV fission of  $U^{238}$  is an order of magnitude larger than at the lower energies. As shown in Fig. 2, the energy distribution for symmetric fission of  $U^{235}$  is independent of the incident neutron energy and the most probable value of  $E_k$  is 158 MeV. Not enough data are available to determine the corresponding energy distribution for 1.5-MeV fission of  $U^{238}$  and the one at 5.6 MeV is very poorly defined. However, it is similar to the  $U^{235}$  distribution, and the most probable value of  $E_k$  is about 158 MeV.

Figures 7 and 8 the data in Table I show that to a first approximation the mass distributions are independent of the incident neutron energy. Under this assumption, the additional kinetic energy of the incident neutron must be equaled by a net increase in the fragment kinetic energy, prompt  $\gamma$ -ray energy, and the energy associated with the prompt fission neutrons. Measurements<sup>27</sup> of  $\bar{\nu}$  show that an increase of 6 MeV in the incident neutron energy increases  $\bar{\nu}$  for  $U^{235}$  by 0.85. This number is very close to the one expected if the fragment excitation energy is increased by 6 MeV.<sup>22</sup> Measurements of  $\bar{E}_k$  for incident neutron energies of 1 to 5 MeV<sup>21</sup> show no significant deviation from the thermal value that cannot be accounted for by the increase in  $\bar{\nu}$ . On the basis of these measurements, it is reasonable to assume that both the prompt  $\gamma$ -ray energy and the fragment kinetic energy prior to neutron emission remain constant. The thermal and 6-MeV data in Table I are in reasonable agreement with these assumptions providing all of  $E_n$  goes to increase the excitation energy of the light fragment. In this case, Eqs. (2) and (6) show that if  $\Delta\nu=0.85$  then  $\Delta\bar{E}_L=-0.9$  MeV,  $\Delta\bar{E}_H=0$ , and  $\bar{\mu}_L$  and  $\bar{\mu}_H$  will shift toward symmetry by 0.5 mass units. The observed values averaged over the three angles are in fair agreement with  $\Delta\bar{E}_L=-1.3 \pm 0.1$  MeV,  $\Delta\bar{E}_H=0.1 \pm 0.2$  MeV, and a shift toward symmetry of 0.6 mass units. When considered alone, these results suggest that the principal difference between fission of  $U^{235}$  by thermal neutrons and 6-MeV neutrons is the addition of 6 MeV to the excitation energy of the light fragment.

<sup>26</sup> J. G. Cuninghame, G. P. Kitt, and E. R. Rae, Nucl. Phys. 27, 154 (1961).

<sup>27</sup> D. S. Mather, P. Fieldhouse, and A. Moat, Phys. Rev. 133, B1403 (1964).

Examination of the dependence of the average single fragment kinetic energy  $E$  on  $\mu$  in Fig. 7 shows that the above description is inadequate. Unfortunately, double-energy measurements alone do not provide enough information to determine the mass dependence of the way the energy is partitioned. Although comparisons of energies averaged over similar mass distributions are straightforward, similar comparisons for particular mass divisions can be misleading because of the interrelation of  $E$  and  $\mu$ .

The observed change in the kinetic energy of the  $i$ th fragment can be written as

$$\Delta E_i = \Delta E_i^* + \Delta \nu_i (E_i^*/m_i^*) + \Delta \mu_i (dE_i/d\mu_i). \quad (8)$$

The first two terms represent a real change in energy while the third term concerns an apparent energy change due to the interrelation of  $E$  and  $\mu$ .  $\Delta \mu$  is defined by the total differential of Eq. (6) and  $dE/d\mu$  is ob-

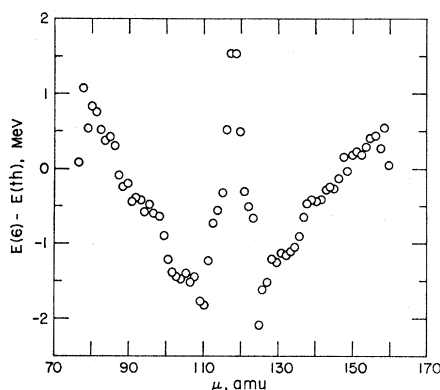


FIG. 9. The difference of the single-fragment energies as a function of the provisional mass for thermal and 6-MeV neutron fission of  $U^{235}$ .

tained from Fig. 7. If the mass dependence of  $\Delta \nu_i$  is known, an energy balance permits the calculation of  $\Delta E_i^*$ . However, even if  $\Delta \nu_i$  is not known, qualitative statements concerning the partition of energy can be made for regions where  $dE/d\mu$  is small enough for the third term to be negligible. For example, at  $\mu=80$  Fig. 7 shows that  $dE/d\mu$  is small, while Fig. 9 shows that  $\Delta E=1.0$  MeV. Since  $\nu$  for thermal fission<sup>9</sup> is very small at this mass value, the increase in  $E$  cannot be due to a decrease in  $\nu$  but must be caused by an increase in  $E_k^*$ . Similarly, at  $\mu=105$ ,  $\Delta E=-1.5$  MeV and  $dE/d\mu$  is still small. If all of  $E_n$  goes to increase  $\nu_i$ ,  $\Delta E$  should be  $-0.9$  MeV. Any greater decrease in  $E$  must be the result of a decrease in  $E_k^*$ . In general, the data in Fig. 9 suggest that for very asymmetric fission, a large part of  $E_n$  is added to  $E_k^*$  while for more nearly symmetric fission the fragment excitation energy is increased by an amount larger than  $E_n$  with a corresponding reduction in  $E_k^*$ .

Similar comparisons of 1.5- and 5.6-MeV fission of  $U^{238}$  give little information because of the larger relative errors associated with the data. Measurements of  $\bar{\nu}$  show that 0.6 additional neutrons<sup>28</sup> are emitted at 5.6 MeV. Inserting this number into Eq. (2) shows that the greatest energy change occurs when the additional neutrons come from the light fragment but even then is only  $-0.6$  MeV. The experimental values are  $\Delta E_L = -1.5 \pm 0.6$  MeV and  $\Delta E_H = -1.3 \pm 0.6$  MeV. The mass dependence of the average single-fragment kinetic energies is shown in Fig. 8. In the region below  $\mu=105$  the two plots are nearly parallel and show no tendency to cross as in the case of thermal and 6-MeV fission of  $U^{235}$ .

<sup>28</sup> I. Asplund-Nilsson, H. Conde, and N. Starfelt, Nucl. Sci. Eng. 20, 527 (1964).